

D. Brömmel,^{1,2} M. Diehl,¹ M. Göckeler,² Ph. Hägler,³ R. Horsley,⁴ Y. Nakamura,⁵
D. Pleiter,⁵ P.E.L. Rakow,⁶ A. Schäfer,² G. Schierholz,^{1,5} H. Stüben,⁷ and J.M. Zanotti⁴
(QCDSF/UKQCD Collaborations)

(Dated: August 20, 2009)

where Δ_\perp is the transverse momentum transfer. The momentum-space GFFs $B_{Tn0}^\pi(t)$ parameterize pion ma-

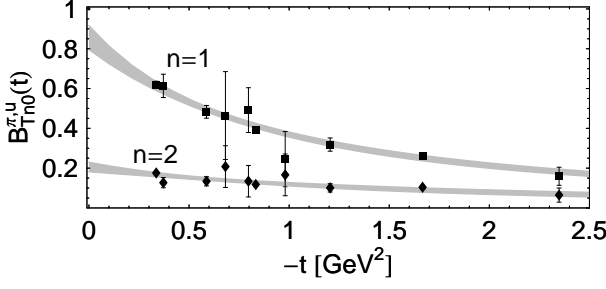


FIG. 2: Lattice results at $\beta = 5.29$ and $m_\pi \approx 600$ MeV for the first two generalized form factors $B_{Tn0}^{\pi,u}(t)$ for up-quarks in the π^+ . The shaded bands show p -pole parameterizations.

trix elements of local tensor quark operators,

$$\langle \pi^+(P') | \mathcal{O}_T^{\mu\nu\mu_1\cdots\mu_{n-1}} | \pi^+(P) \rangle = \mathcal{AS} \frac{\bar{P}^\mu \Delta^\nu - \Delta^\mu \bar{P}^\nu}{m_\pi} \times \sum_{\substack{i=0 \\ \text{even}}}^{n-1} \Delta^{\mu_1} \cdots \Delta^{\mu_i} \bar{P}^{\mu_{i+1}} \cdots \bar{P}^{\mu_{n-1}} B_{Tni}^\pi(t) \quad (4)$$

with $\bar{P} = \frac{1}{2}(P' + P)$, $\Delta = P' - P$ and $t = \Delta^2$. Here \mathcal{AS} denotes symmetrization in ν, \dots, μ_{n-1} followed by anti-symmetrization in μ, ν and subtraction of traces in all index pairs. The tensor operators are given by

$$\mathcal{O}_T^{\mu\nu\mu_1\cdots\mu_{n-1}} = \mathcal{AS} \bar{q} i\sigma^{\mu\nu} i\overleftrightarrow{D}^{\mu_1} \cdots i\overleftrightarrow{D}^{\mu_{n-1}} q \quad (5)$$

with $\overleftrightarrow{D} = (\vec{D} - \overleftarrow{D})/2$ and all fields taken at space-time point $z = 0$. The analogous matrix elements of local vector quark operators are parameterized by $A_{n0}^\pi(t)$ as specified in [5]. For definiteness we consider in the following $A_{n0}^{\pi,u}(t)$ and $B_{Tn0}^{\pi,u}(t)$ for up-quarks in a π^+ . Their counterparts for down-quarks and for π^- or π^0 readily follow from isospin invariance [2], since Wilson fermions preserve flavor symmetry. We note that $A_{10}^{\pi,u}(t)$ is identical to the electromagnetic pion form factor $F_\pi(t)$, which we investigated in detail in [6].

Lattice QCD results.— Based on our simulations with Wilson gluons and dynamical, non-perturbatively $\mathcal{O}(a)$ improved Wilson fermions with $n_f = 2$, we have evaluated the matrix elements in Eq. (4) for $n = 1, 2$ and momentum transfers up to $-t \approx 3 \text{ GeV}^2$. Configurations were generated at four different couplings $\beta = 5.20, 5.25, 5.29, 5.40$ with up to five different $\kappa = \kappa_{\text{sea}}$ values per β , on lattices of sizes $V \times T = 16^3 \times 32$ and $24^3 \times 48$. We have set the lattice scale a using a Sommer parameter of $r_0 = 0.467 \text{ fm}$ [7]. The pion masses are as low as 400 MeV, spatial volumes are as large as $(2.1 \text{ fm})^3$, and lattice spacings are below 0.1 fm (see [6] for a list of lattice parameters). The computationally demanding disconnected contributions present for even n are not included. For the tensor GFFs B_{Tn0}^π we expect them to be small in the physical limit, since they require a chirality flip on a quark line and are thus suppressed by the quark mass [8]. All results were transformed to the $\overline{\text{MS}}$ scheme

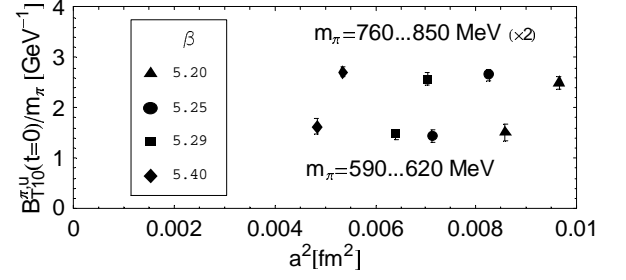


FIG. 3: Study of discretization errors in $B_{T10}^{\pi,u}(t=0)/m_\pi$.

at a scale of 4 GeV^2 using non-perturbative renormalization [9]. Further information on the computation of GFFs in lattice QCD can be found, e.g., in [6, 10], and details of the present analysis will be given in [11].

As an example we show in Fig. 2 the t dependence of $B_{T(n=1,2)0}^{\pi,u}$ at $\beta = 5.29$ and $m_\pi \approx 600$ MeV. The extrapolation to the forward limit $t = 0$ requires a parameterization of the t dependence of the lattice results. As the statistics and t range of our data is not yet sufficient for sophisticated multi-parameter fits, we use a standard p -pole form $F(t) = F_0/[1 - t/(p m_p^2)]^p$, where the forward value $F_0 = F(t=0)$ and the p -pole mass m_p are free parameters for each GFF. Good fits are obtained in a wide range of p , with a preference for relatively low values. On the other hand, a regular behavior of $\rho^n(b_\perp, s_\perp)$ in the limit $b_\perp \rightarrow 0$ (which is of course inaccessible in a lattice calculation) requires $p > 3/2$ for $B_{Tn0}^{\pi,u}(t)$ [4]. We therefore take $p = 1.6$ in the following. For the examples in Fig. 2 we obtain $B_{T10}^{\pi,u}(t=0) = 0.856(60)$ with $m_p = 0.949(57) \text{ GeV}$, and $B_{T20}^{\pi,u}(t=0) = 0.206(24)$ with $m_p = 1.239(30) \text{ GeV}$. We stress that our final results show only a mild dependence on the chosen value of p . Taking, e.g., $p = 2$, which gives the power behavior for $t \rightarrow -\infty$ expected from dimensional counting, changes our fits of $B_{Tn0}^{\pi,u}$ by less than the statistical errors even beyond the region $-t < 3 \text{ GeV}^2$ where we have data [11].

Before discussing potential discretization and finite size effects as well as the pion mass dependence of our results we note that, due to the prefactor m_π^{-1} in the parameterization (4), the GFFs $B_{Tn0}^\pi(t)$ must vanish like m_π for $m_\pi \rightarrow 0$ [2]. This is also required to ensure that the densities in Eq. (1) stay positive and finite in the chiral limit. In the following we therefore consider the ratio B_{Tn0}^π/m_π , which tends to a constant at $m_\pi = 0$.

Figure 3 shows the dependence of $B_{T10}^{\pi,u}(t=0)/m_\pi$ on the lattice spacing a for two ranges of pion masses, where we have excluded those lattice data points which are most strongly affected by finite volume corrections (see below). We conclude that discretization errors are smaller than the statistical errors and neglect any dependence of the GFFs on a in the following analysis.

Figure 4 shows the volume dependence of $B_{T10}^{\pi,u}(t=0)/m_\pi$ for three different ranges of m_π . The finite volume corrections to the matrix elements

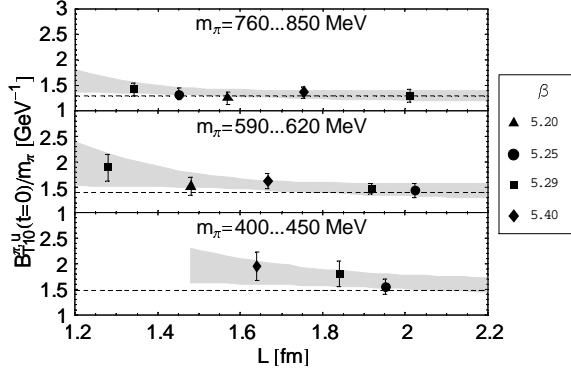


FIG. 4: Study of finite size effects of $B_{T10}^{\pi,u}(t=0)/m_{\pi}$. Shaded bands represent a combined fit (restricted to $m_{\pi}L > 3$) in m_{π} and L as described in the text. The dashed lines show the infinite-volume limit of the fit.

with $n = 1, 2$ in Eq. (4) are known to leading order in chiral perturbation theory (ChPT) [12]. For $m_{\pi}L \gg 1$ the leading correction to $B_{Tn0}^{\pi,u}(t=0)/m_{\pi}$ is proportional to $m_{\pi}^2 \exp(-m_{\pi}L)$ up to powers of $(m_{\pi}L)^{-1/2}$, where L is the spatial extent of the lattice. Although our analysis includes pion masses as low as 400 MeV, we feel that a quantitative application of the chiral expansion requires lattice computations at even lower values of m_{π} and probably the inclusion of higher-order terms. We take however the result of [12] as a guide to estimate the L dependence of our lattice data, fitting $B_{T10}^{\pi,u}(t=0)/m_{\pi}$ to the form $c_0 + c_1 m_{\pi}^2 + c_2 m_{\pi}^2 \exp(-m_{\pi}L)$. This fit, represented by shaded bands in Fig. 4, gives $B_{T10}^{\pi,u}(t=0) = 1.47(18) \text{ GeV}^{-1}$ at $L = \infty$ and $m_{\pi} \sim 440 \text{ MeV}$, compared to $B_{T10}^{\pi,u}(t=0) = 1.95(27) \text{ GeV}^{-1}$ at $L \sim 1.65 \text{ fm}$ as represented by the diamond in the lowest panel of Fig. 4. The typical corrections for $B_{T20}^{\pi,u}(t=0)/m_{\pi}$ are similar. Within present statistics, we do not see a clear volume dependence of the corresponding p -pole masses for $n = 1, 2$.

The pion mass dependence of $B_{Tn0}^{\pi,u}(t=0)/m_{\pi}$ is shown in Fig. 5. The darker shaded bands show fits based on the ansatz we just described. Data points and error bands have been shifted to $L = \infty$. For $m_{\pi} = 140 \text{ MeV}$ we obtain $B_{T10}^{\pi,u}(t=0)/m_{\pi} = 1.54(24) \text{ GeV}^{-1}$ with $m_p = 0.756(95) \text{ GeV}$, and $B_{T20}^{\pi,u}(t=0)/m_{\pi} = 0.277(71) \text{ GeV}^{-1}$ with $m_p = 1.130(265) \text{ GeV}$, where in both cases we have set $p = 1.6$. The errors of the forward values include the uncertainties from finite volume effects. The light shaded bands in Fig. 5 show fits restricted to $m_{\pi} < 650 \text{ MeV}$ using 1-loop ChPT [2] plus the volume dependent term $c_2 m_{\pi}^2 \exp(-m_{\pi}L)$. We note that the ChPT-extrapolation gives larger values for $B_{T10}^{\pi,u}(t=0)$ at the physical point than the linear extrapolation in m_{π}^2 .

To compute the lowest two moments of the density in Eq. (1) we further need the GFFs $A_{n0}^{\pi}(t)$ with $n = 1, 2$. For $A_{10}^{\pi,u}(t) = F_{\pi}(t)$ we refer to our results in [6]. A detailed analysis of $A_{20}^{\pi,u}(t)$ will be presented in [11], and first results are given in [5]. We fit $A_{n0}^{\pi,u}(t)$ to a

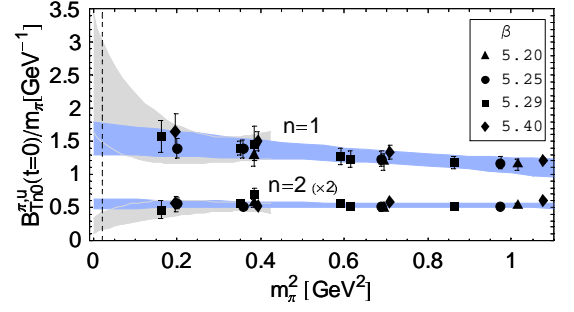


FIG. 5: Pion mass dependence of $B_{Tn0}^{\pi,u}(t=0)/m_{\pi}$. The shaded bands represent fits as explained in the text.

p -pole parameterization with $p = 1$, which provides an excellent description of the lattice data and is consistent with power counting for $t \rightarrow -\infty$. Fourier transforming the parameterizations of the momentum-space GFFs we obtain the densities $\rho^n(b_{\perp}, s_{\perp})$. In Fig. 6 we show $\rho^{n=1}(b_{\perp}, s_{\perp})$ for up-quarks in a π^+ together with corresponding profile plots for fixed b_x . Compared to the unpolarized case on the left, the right-hand side of Fig. 6 shows strong distortions for transversely polarized quarks and thus a pronounced spin structure. The difference between $p = 1.6$ and $p = 2$ for $B_{Tn0}^{\pi,u}$ is negligible within errors. The negative values of the density on the lower right in Fig. 6, obtained for the maximal values of $B_{T10}^{\pi,u}$ from the chiral extrapolations in Fig. 5, are unphysical. They show that 1-loop ChPT cannot be regarded as quantitatively reliable in this case and provides only a rough idea of the uncertainties related to the chiral extrapolation. From Eq. (1) we obtain an average transverse shift

$$\langle b_{\perp}^y \rangle_n = \frac{\int d^2 b_{\perp} b_{\perp}^y \rho^n(b_{\perp}, s_{\perp})}{\int d^2 b_{\perp} \rho^n(b_{\perp}, s_{\perp})} = \frac{1}{2m_{\pi}} \frac{B_{Tn0}^{\pi,u}(t=0)}{A_{n0}^{\pi,u}(t=0)} \quad (6)$$

in the y direction for a transverse quark spin $s_{\perp} = (1, 0)$ in the x direction. Our lattice results give $\langle b_{\perp}^y \rangle_1 = 0.151(24) \text{ fm}$ and $\langle b_{\perp}^y \rangle_2 = 0.106(28) \text{ fm}$.

Let us compare our results for B_{Tn0}^{π} with those for the analogous GFFs \bar{B}_{Tn0} that describe the dipole-like distortion in the density of transversely polarized quarks in an unpolarized nucleon. The corresponding average transverse shift is $\langle b_{\perp}^y \rangle_n = \bar{B}_{Tn0}(t=0)/(2m_N A_{n0}(t=0))$, where $A_{n0}(t=0)$ is the n -th moment of the unpolarized quark distribution. With the lattice results of [3] we find $\langle b_{\perp}^y \rangle_1 = 0.154(6) \text{ fm}$ and $\langle b_{\perp}^y \rangle_2 = 0.101(8) \text{ fm}$ for up-quarks in the proton. Remarkably, the distortion in the distribution of a transversely polarized up-quark is within errors of the same strength in a π^+ and in the proton. An explanation of this finding has recently been proposed in the framework of quark models [13].

The moments of the GPDs E_T^{π} in the pion and \bar{E}_T in the nucleon can be connected with the respective Boer-Mulders functions, which describe the correlation between transverse spin and intrinsic transverse momentum of quarks in an unpolarized hadron [14]. They lead, e.g.,

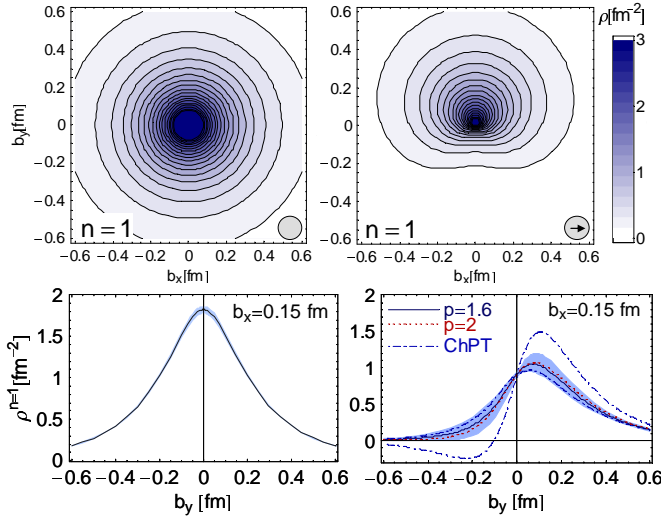


FIG. 6: The lowest moment of the densities of unpolarized (left) and transversely polarized (right) up-quarks in a π^+ together with corresponding profile plots. The quark spin is oriented in the transverse plane as indicated by the arrow. The error bands in the profile plots show the uncertainties in $B_{T10}^{\pi,u}(t=0)/m_\pi$ and the p -pole masses at m_π^{phys} from a linear extrapolation. The dashed-dotted lines show the uncertainty from a ChPT-extrapolation (light shaded band in Fig. 5).

to azimuthal asymmetries in semi-inclusive deep inelastic scattering (SIDIS) and in Drell-Yan lepton pair production. The density of quarks with transverse momentum k_\perp and transverse spin s_\perp in a π^+ is given by

$$f(x, k_\perp, s_\perp) = \frac{1}{2} \left[f_1^\pi(x, k_\perp^2) + \frac{s_\perp^i \epsilon^{ij} k_\perp^j}{m_\pi} h_1^{\pi\perp}(x, k_\perp^2) \right] \quad (7)$$

in terms of the unpolarized distribution f_1^π and the Boer-Mulders function $h_1^{\pi\perp}$. We notice the close similarity between (7) and the impact parameter density (1), but emphasize that k_\perp and b_\perp are *not* Fourier conjugate variables. A dynamical relation between k_\perp and b_\perp dependent densities was proposed in [15] and implies $h_1^{\perp,\pi} \sim -E_T^\pi$ for the distribution appearing in SIDIS—we recall that $h_1^{\perp,\pi}$ is time reversal odd and thus enters with opposite signs in SIDIS and Drell-Yan production [16]. With this relation, our results for B_{Tn0}^π imply that the Boer-Mulders function for up-quarks in a π^+ is large and negative, and that its ratio to the unpolarized distribution is similar for up-quarks in a π^+ and in a proton.

Conclusions.— We have calculated the first two moments of the quark tensor GPD E_T^π in the pion. We find that the spatial distribution of quarks is strongly distorted if they are transversely polarized, revealing a non-trivial spin structure of the pion. The effect has

the same sign and very similar magnitude as the corresponding distortion in the nucleon [3]. Assuming the relation between impact parameter and transverse momentum densities proposed in [15] this suggests that all Boer-Mulders functions for valence quarks may be alike, as argued in [13]. The large size of the effect might give new insight into the mechanism responsible for the large $\cos(2\phi)$ azimuthal asymmetry observed in unpolarized πp Drell-Yan production, which is sensitive to the product $h_1^{\perp,\pi} h_1^\perp$ [17]. It motivates future studies of azimuthal asymmetries in unpolarized πp and polarized πp^\dagger Drell-Yan production at COMPASS, the latter giving rise to a $\sin(\phi + \phi_S)$ asymmetry sensitive to $h_1^{\perp,\pi} h_1$, where h_1 is the quark transversity distribution in the nucleon [18].

The numerical calculations have been performed on the Hitachi SR8000 at LRZ (Munich), apeNEXT and APEmille at NIC/DESY (Zeuthen) and BlueGene/Ls at NIC/FZJ (Jülich), EPCC (Edinburgh) and KEK (by the Kanazawa group as part of the DIK research program). This work was supported by DFG (Forschergruppe Gitter-Hadronen-Phänomenologie and Emmy-Noether program), by HGF (contract No. VH-NG-004) and by EU I3HP (contract No. RII3-CT-2004-506078).

* Electronic address: phaegler@ph.tum.de

- [1] M. Burkardt, Phys. Rev. D **62**, 071503 (2000) [Erratum ibid. D **66**, 119903 (2002)]; Int. J. Mod. Phys. A **18**, 173 (2003); D. E. Soper, Phys. Rev. D **15**, 1141 (1977).
- [2] M. Diehl, A. Manashov and A. Schäfer, Phys. Lett. B **622**, 69 (2005); Eur. Phys. J. A **31** 335 (2007).
- [3] M. Göckeler *et al.*, Phys. Rev. Lett. **98**, 222001 (2007).
- [4] M. Diehl and Ph. Hägler, Eur. Phys. J. C **44**, 87 (2005).
- [5] D. Brömmel *et al.*, PoS **LAT2005**, 360 (2006).
- [6] D. Brömmel *et al.*, Eur. Phys. J. C **51**, 335 (2007).
- [7] A. Ali Khan *et al.*, Phys. Rev. D **74**, 094508 (2006); C. Aubin *et al.*, Phys. Rev. D **70** (2004) 094505.
- [8] M. Göckeler *et al.*, Phys. Lett. B **627**, 113 (2005).
- [9] G. Martinelli *et al.*, Nucl. Phys. B **445**, 81 (1995); M. Göckeler *et al.*, Nucl. Phys. B **544**, (1999) 699.
- [10] M. Göckeler *et al.*, Phys. Rev. Lett. **92**, 042002 (2004); Ph. Hägler *et al.*, Phys. Rev. D **68**, 034505 (2003).
- [11] D. Brömmel *et al.*, in preparation.
- [12] A. Manashov and A. Schäfer, arXiv:0706.3807.
- [13] M. Burkardt and B. Hannafious, Phys. Lett. B **658**, 130 (2008).
- [14] D. Boer and P. J. Mulders, Phys. Rev. D **57**, 5780 (1998).
- [15] M. Burkardt, Phys. Rev. D **72**, 094020 (2005); S. Meissner, A. Metz and K. Goeke, Phys. Rev. D **76**, 034002 (2007).
- [16] J. C. Collins, Phys. Lett. B **536**, 43 (2002).
- [17] D. Boer, Phys. Rev. D **60** (1999) 014012.
- [18] A. Sissakian *et al.*, Eur. Phys. J. C **46**, 147 (2006); A. Bianconi and M. Radici, Phys. Rev. D **73**, 114002 (2006).